Probing sizes and shapes of nobelium isotopes by laser spectroscopy

S. Raeder,[1,2,*] D. Ackermann,[3,2] H. Backe,[4] R. Beerwerth,[5,6] J. C. Berengut,[7] M. Block,[1,2,8] A. Borschevsky,[9]

B. Cheal,[10] P. Chhetri,[2,11] Ch.E. Düllmann,[1,2,8] V.A. Dzuba,[7] E. Eliav,[12] J. Even,[13] R. Ferrer,[14]

V.V. Flambaum,[1,7] S. Fritzsche,[5,6] F. Giacoppo,[1,2] S. Götz,[1,8] F.P. Heßberger,[1,2] M. Huyse,[14] U. Kaldor,[12]

O. Kaleja,[2,15,†] J. Khuyagbaatar,[1,2] P. Kunz,[16] M. Laatiaoui,[1,2] F. Lautenschläger,[2,11] W. Lauth,[4]

A.K. Mistry,[1,2] E. Minaya Ramirez,[17] W. Nazarewicz,[18] S.G. Porsev,[19,20] M.S. Safronova,[19,21]

U.I. Safronova,[22] B. Schuetrumpf,[15,2] P. Van Duppen,[14] T. Walther,[11] C. Wraith,[10] and A. Yakushev[1,2]

[1]Helmholtz-Institut Mainz, 55128 Mainz, Germany.
[2]GSI Helmholtzzentrum für Schwerionenforschung GmbH, 64291 Darmstadt, Germany.
[3]GANIL, CEA/DRF-CNRS/IN2P3, Bd. Becquerel, BP 55027, F-14076 Caen, France
[4]Institut für Kernphysik, Johannes Gutenberg Universität, 55128 Mainz, Germany.
[5]Helmholtz-Institut Jena, 07743 Jena, Germany.
[6]Theoretisch-Physikalisches Institut, Friedrich-Schiller-Universität Jena, 07743 Jena, Germany
[7]School of Physics, University of New South Wales, Sydney 2052, Australia
[8]Institut für Kernchemie, Johannes Gutenberg Universität, 55128 Mainz, Germany.
[9]Van Swinderen Institute, University of Groningen, 9747 AG Groningen, The Netherlands
[10]Department of Physics, University of Liverpool, L69 7ZE Liverpool, UK.
[11]Institut für Angewandte Physik, Technische Universität Darmstadt, 64289 Darmstadt, Germany.
[12]School of Chemistry, Tel Aviv University, 69978 Tel Aviv, Israel
[13]KVI CART, University of Groningen, 9747 AA Groningen, The Netherlands.
[14]KU Leuven, Instituut voor Kern- en Stralingsfysica, 3001 Leuven, Belgium.
[15]Institut für Kernphysik, Technische Universität Darmstadt, 64289 Darmstadt, Germany.
[16]TRIUMF, 4004 Wesbrook Mall, Vancouver, BC V6T 2A3, Canada.
[17]Institut de Physique Nucléaire Orsay,91406 Orsay, France.
[18]Department of Physics and Astronomy and FRIB Laboratory,
Michigan State University, East Lansing, Michigan 48824, USA.
[19]Department of Physics and Astronomy, University of Delaware, Newark, Delaware 19716, USA
[20]Petersburg Nuclear Physics Institute of NRC "Kurchatov Institute", Gatchina, Leningrad District 188300, Russia
[21]Joint Quantum Institute, NIST and the University of Maryland, College Park, Maryland, USA
[22]Physics Department, University of Nevada, Reno, Nevada 89557, USA
(Dated: April 7, 2018)

Until recently, ground state nuclear moments of the heaviest nuclei could only be inferred from nuclear spectroscopy, where model assumptions are required. Laser spectroscopy in combination with modern atomic structure calculations is now able to probe these moments directly, in a comprehensive and nuclear model-independent way, for the first time. Here we report on unique access to the differential mean-square charge radii of ^{252,253,254}No, and therefore to changes in nuclear size and shape. State-of-the-art nuclear density functional calculations describe well the changes in nuclear charge radii in the region of the heavy actinides, indicating an appreciable central depression in the deformed proton density distribution in ^{252,254}No isotopes. Finally, the hyperfine splitting of ^{253}No was evaluated enabling a complementary measure of its (quadrupole) deformation, as well as an insight into the neutron single-particle wave function via the nuclear spin and magnetic moment.

The heaviest elements owe their existence to a subtle balance between the attractive nuclear force and the Coulomb repulsion. The attractive force leads to strong shell effects that increase the binding energy and thus the half-life by more than fifteen orders of magnitude compared to early expectations [1]. Coulomb rearrangement plays a key role in superheavy nuclei resulting in a central depression in the density distribution and may even result in bubble nuclei (see Ref. [2] and references therein). Unfortunately, measurements of charge or matter radii have stopped short of transfermium nuclei. The nuclei between the spherical ^{208}Pb and a predicted island of enhanced stability in the region of the superheavy nuclei [3] are expected to be deformed [4]. Evidence for the deformation is provided by the observation of K-isomers [5, 6]

and from rotational bands in nuclear decay spectroscopy, for example, in ^{254}No [7, 8] or ^{256}Rf [9]. The deformation parameters and other nuclear properties such as the magnetic moment are then derived based on a model-dependent interpretation of such rotational levels built on the nuclear ground state [10]. Laser spectroscopy, on the contrary, enables probing the nuclear ground state directly: the atomic spectra of different isotopes reveal information on the nuclear spin, nuclear moments and differential nuclear mean-charge radii [11]. Atom-at-a-time laser spectroscopy of the heavy actinide element nobelium (No, $Z = 102$), in which the $^1S_0 \rightarrow {}^1P_1$ transition at an excitation energy of $\bar{\nu}_1 = 29{,}961.457\,\text{cm}^{-1}$ was identified [12], was a prerequisite for our studies. Here, we report detailed laser spectroscopy on the nobelium

isotopes ^{252,253,254}No from which, in combination with state-of-the-art atomic calculations, information on the underlying nuclear structure is obtained.

The RAdiation Detected Resonance Ionization Spectroscopy (RADRIS) technique [13, 14] employs a two-step photo-ionization process along with an unambiguous identification via radioactive decay detection. The nobelium isotopes ^{252,253,254}No were produced in the two neutron evaporation channel of the complete-fusion of ^{48}Ca with ^{206,207,208}Pb with cross-sections of $0.5\,\mu$b (^{252}No), $1.3\,\mu$b(^{253}No), and $2\,\mu$b (^{254}No) [15]. The ^{48}Ca beam was provided by the linear accelerator (UNILAC) of GSI Helmholtzzentrum für Schwerionenforschung in Darmstadt with average beam currents of 0.7 particle μA (about 4.4×10^{12} particles per second). The fusion-evaporation products, recoiling from the PbS targets, with a thickness of about $440\,\mu$g/cm^2, were separated in-flight from the primary beam by the Separator for Heavy Ion reaction Products (SHIP)[16]. At the best four ions per second were injected into a buffer-gas stopping cell installed at the focal plane of SHIP. A $3.5\,\mu$m thick, aluminized Mylar foil window separated the gas environment of the gas cell from the high vacuum of SHIP. The ions were thermalized in $95\,$mbar ultrahigh-purity argon gas (99.9999%), accumulated, and neutralized on a tantalum catcher filament. For a short time during every measurement the primary beam was chopped out before the filament was heated to temperatures of about $1050°$C at which neutral nobelium atoms are efficiently released [17]. For best performance, we varied the collection time with respect to the half-life of the isotope [18]: $3\,$s for ^{252}No ($T_{1/2}=2.4\,$s), $37\,$s for ^{253}No ($T_{1/2}=97\,$s), and $25\,$s for ^{254}No ($T_{1/2}=51.2\,$s). The released atoms were probed by two laser beams of suitable wavelengths in a two-step photo-ionization scheme (see inset in Fig. 1). The second step was set to a wavelength $\lambda_2 = 351\,$nm such that the total excitation energy exceeded the first ionization potential (IP) for non-resonant ionization, with a pulse energy density of $2\,$mJ/cm^2. This laser efficiently ionized atoms excited to the ^{1}P$_1$ state but also the fraction of atoms where the population that was transferred to a long-lived atomic state by gas collisions [19]. Ions created by resonant laser ionization were guided by electrostatic potentials to a silicon detector and identified by their characteristic α-decay energy or additionally by the detection of high energetic fission fragments in the case of ^{252}No. This method enables a selective and efficient laser spectroscopy, resulting in a total efficiency of $3.3(1.0)\%$ for ^{252}No [12], $8.2(2.5)\%$ for ^{253}No, and $6.4(1.0)\%$ for ^{254}No [12]. To probe nuclear properties of the nobelium isotopes, we scanned the first excitation step around the ^{1}P$_1$ level with a resolution of about $4\,$GHz (FWHM) limited mainly by the laser bandwidth ($1.2\,$GHz) and collisional broadening ($4\,$GHz). For ^{252}No we operated the laser with an increased laser bandwidth of $5.5\,$GHz, which reduced the final resolution, but also reduced the number

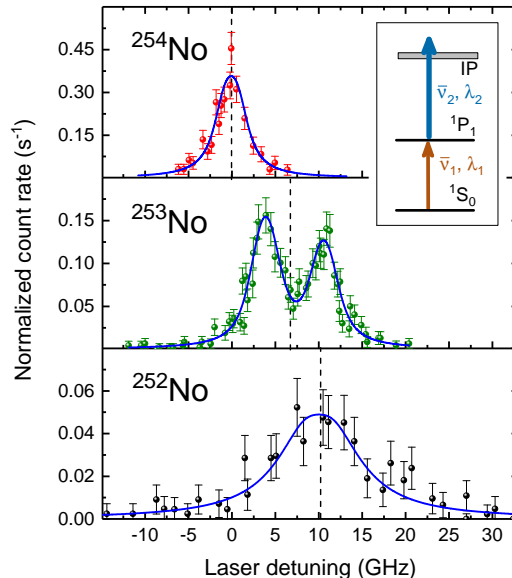FIG. 1. Measured excitation spectra of the ^{1}P$_1$ level for the isotopes ^{254}No, ^{253}No, and ^{252}No with a best fit to the data (solid line). The dashed line represents the center of each resonance while the solid vertical lines in the ^{253}No spectrum indicate the position and strength of the individual hyperfine structure components with total angular momentum $F = 7/2$, $9/2$, and $11/2$ at $3.99\,$GHz, $4.10\,$GHz, and $10.74\,$GHz, respectively. The inset shows a schematic ionization scheme.

of scan steps for a more efficient beamtime usage. The measured spectra are shown in Fig. 1.

Besides a shift of the resonance centroid of the individual isotopes, the spectrum of the odd-mass isotope ^{253}No additionally features a splitting. This originates from the hyperfine interaction that leads to a coupling of the electron angular momentum J with the nuclear spin I. The resulting splitting ΔE_{HFS} depends on the total angular momentum F and the hyperfine coupling constants $A_{\mathrm{HFS}} = \mu \frac{B_e}{IJ}$ and $B_{\mathrm{HFS}} = eQ_s \left\langle \frac{\partial^2 V}{\partial z^2} \right\rangle$, where μ and Q_s are the magnetic dipole moment and the spectroscopic quadrupole moment of the nucleus, respectively. The magnetic dipole moment μ couples to the magnetic field created by the electron orbital at the nucleus B_e while Q_s links to the electric field gradient at the nucleus $\left\langle \frac{\partial^2 V}{\partial z^2} \right\rangle$ with the elementary charge e. These atomic parameters, which are isotope-independent and connect atomic observables to nuclear properties, were obtained from state-of-the-art atomic calculations. Different theoretical approaches were applied to calculate these parameters for nobelium: configuration interaction (CI) with the single-double coupled cluster method (CI+All orders) [20], CI combined with many-body perturbation theory (MBPT) [21–23], and relativistic Fock space coupled cluster (FSCC) [24] as well as multi configuration Dirac-Fock (MCDF) calculations [25, 26]. The

TABLE I. Summary of the atomic calculations, the experimental results, and the extracted nuclear parameters for ^{252,253,254}No. The values of the calculated HFS coupling parameters B_e/J and $e\left\langle\partial^2 V/\partial z^2\right\rangle$, the field shift constant F_s and the mass shift constant M have been calculated with different techniques in this work and are presented together with the spectroscopic results obtained in the experiment. From these values the nuclear magnetic moment μ, the spectroscopic quadrupole moment Q_s and the changes in mean square charge radii $\delta\langle r^2\rangle$ between the nuclei are extracted. μ_N denotes the nuclear magneton.

	Hyperfine splitting for ^{253}No		Isotope shift	
Atomic calculations	B_e/J $(\mathrm{GHz}\cdot I/\mu_\mathrm{N})$	$e\left\langle\partial^2 V/\partial z^2\right\rangle$ $(\mathrm{GHz}/\mathrm{eb})$	F_s $(\mathrm{GHz}/\mathrm{fm}^2)$	M $(\mathrm{GHz}\cdot\mathrm{amu})$
CI+All orders	$-6.3(0.9)^\dagger$	$0.486(70)^\dagger$	$-95.8(7.0)^\dagger$	
CI+MBPT	$-7.1(1.0)$	$0.503(75)$	$-104(10)$	
CIPT	$-7.4(1.2)$	$0.624(90)$	$-94(25)$	
FSCC		$0.465(70)^\dagger$	$-99(15)$	
MCDF	$-4.1(1.8)$	$0.444(75)$	$-113(25)$	$1044(400)^\dagger$

† values used to deduce nuclear ground-state parameters.

Spectroscopic results	A_HFS (GHz)	B_HFS (GHz)	$\delta\nu^{254,253}$ (GHz)	$\delta\nu^{254,253}$ (GHz)
	$0.734(46)$	$2.82(69)$	$6.72(18)$	$10.08(69)$

Nuclear properties	$\mu(\mu_\mathrm{N})$	Q_s (eb)	$\delta\langle r^2\rangle^{254,253}$ (fm^2)	$\delta\langle r^2\rangle^{254,252}$ (fm^2)
	$-0.527(33)(75)$	$+5.9(1.4)(0.9)$	$-0.070(2)(5)$	$-0.105(7)(7)$

results of these calculations are summarized in Table I. In general, the different methods agree with one another to within about 20%. By applying a newly developed method which is based on the CI technique but treats high-energy states perturbatively (CIPT method) [27], the influence of configuration mixing on the investigated $^1P_1$ level was evaluated at the cost of an increased uncertainty. This allowed to verify and exclude a possible scenario of a strong mixing with core excitations. From systematic investigations of chemical elements with similar electronic configurations, the most accurate values for the hyperfine coupling parameter B_e/J and the isotope field shift constant F_s are expected for CI(+All orders) calculations. Thus, these results were taken for extracting the nuclear properties. CI(+All orders) calculations and FSCC calculations provide the same uncertainty for the parameter $e\left\langle\partial^2 V/\partial z^2\right\rangle$ for which an average value of $0.476(70)\,\mathrm{GHz/eb}$ was used in the evaluation.

From a total of three HFS transitions to the $^1P_1$ state in ^{253}No only two were resolved. The splitting of the hyperfine structure (HFS) levels depends on the nuclear spin. Under the assumption of a prolate shape of the ^{253}No nucleus, and by considering the sign of the extracted magnetic moment and the χ^2 of the fit, a nuclear spin of $I(^{253}\mathrm{No}) = 9/2$, which was used later on in the evaluation, is favoured over $I(^{253}\mathrm{No}) = 7/2$. This result independently substantiates conclusions from nuclear spectroscopy [28, 29]. The hyperfine coupling constants $A_\mathrm{HFS} = 0.734(46)\,\mathrm{GHz}$ and $B_\mathrm{HFS} = 2.82(67)\,\mathrm{GHz}$ for ^{253}No were derived from a χ^2-minimization of a rate equation model to the experimental data which includes saturation effects from the pulsed laser excitation on the individual intensities [30]. For ^{253}No, which features an even proton number, $Z = 102$, and an odd neu-

tron number, $N = 151$, the nuclear magnetic properties arise mainly from the unpaired neutron. Our experimental determination of the magnetic dipole moment to $\mu(^{253}\mathrm{No}) = -0.527(33)(75)\,\mu_\mathrm{N}$ therefore enables probing nuclear shell model predictions of the underlying nuclear single neutron wave function. The first parenthesis refers to the statistical uncertainty (1σ) and the second parenthesis refers to the uncertainty from atomic calculations. The nuclear magnetic moment of the band-head of a rotational band in a well-deformed nucleus, such as expected in the case of ^{253}No, can be written as

$$\mu/\mu_\mathrm{N} = g_K\frac{I^2}{I+1} + g_R\frac{I}{I+1} \quad . \tag{1}$$

It depends on the rotational g-factor $0.7\cdot Z/A \leq g_R \leq Z/A$ [31] and the single-particle intrinsic g-factor g_K, which so far was calculated from nuclear models. From our data on the magnetic moment, an average value of $g_K^\mathrm{exp} = -0.22(5)$ is extracted which considers the stated range of g_R. This result is consistent with a calculated value of $g_K = -0.25$ reported in [29, 32] for the $I(^{253}\mathrm{No}) = 9/2^-[734]$ ground state configuration while it disagrees with a different calculated value $g_K = -0.12$, reported in [33].

From the B_HFS-value of the HFS splitting, a spectroscopic quadrupole moment of $Q_\mathrm{s}(^{253}\mathrm{No}) = +5.9(1.4)(0.9)\,\mathrm{eb}$ is deduced indicating a strong prolate deformation of the ^{253}No nucleus, in agreement with the observation of K-isomers in nobelium isotopes [5]. From our result an intrinsic quadrupole moment of $Q_0(^{253}\mathrm{No}) = +10.8(2.6)(1.7)\,\mathrm{eb}$ is extracted. This value is comparable with the shell model-dependent value of $Q_\mathrm{s}(^{254}\mathrm{No}) = +13.1\,\mathrm{eb}$ [32, 33], obtained from the moment of inertia in the rotational
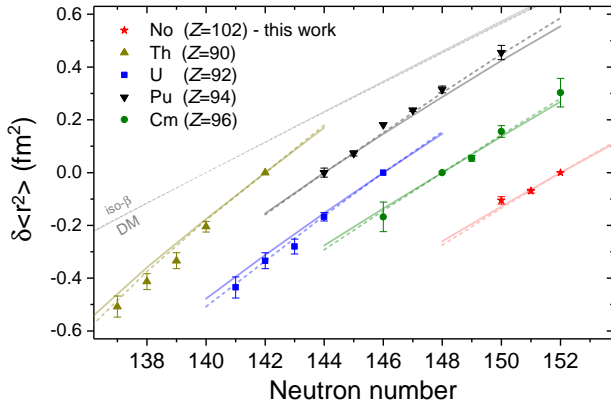
FIG. 2. The change in the nuclear mean square charge radii $\delta\langle r^2\rangle$, for $^{252-254}$No and even Z actinide nuclei starting from thorium, is plotted as a function of the neutron number with arbitrary offset. For each element the DFT calculations with two Skyrme energy density functionals, UNEDF1 [34] (dashed line) and SV-min [35] (solid line), are shown. The gray area indicates the slope according to the iso-beta using a schematic droplet model when assuming constant deformation for the actinide elements referenced to $N = 138$.
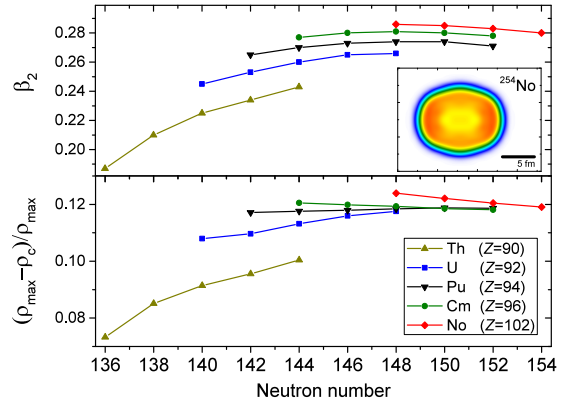
FIG. 3. Upper panel: deformation parameter β_2 for different even-even isotopes of Th, U, Pu, Cm, and No obtained from the DFT calculations with the UNEDF1 functional. The inset figure shows the calculated proton distribution of ^{254}No from highest density (red) to low density (blue). Lower panel: relative depth of the central depression.

band built on the ground state of ^{254}No [7, 8]. These values indicate a constant deformation in the isotope chain of nobelium around the neutron shell closure $N = 152$.

Information on the deformation of the even mass nuclei ^{252,254}No with zero nuclear spin can be obtained from laser spectroscopic measurements through a complementary route. The change in deformation is manifested in the isotope shift (IS) of an atomic transition $\delta\nu^{A,A'} = \nu^{A'} - \nu^A$ between two isotopes A and A' with masses m_A and $m_{A'}$. IS values of $\delta\nu^{254,253} = 6.72(18)\,\mathrm{GHz}$ and $\delta\nu^{254,252} = 10.08(69)\,\mathrm{GHz}$ were measured in this work. The IS arises from a mass shift, with a mass shift constant M, and a field shift, with a field shift constant F_s. The latter is the dominant factor for heavy elements and is characterized by the density of the electron wave function inside the nucleus. The IS is related to the change in the nuclear mean square charge radius $\delta\langle r^2\rangle^{A,A'}$ by

$$\delta\nu^{A,A'} = \frac{m^A - m^{A'}}{m^A \cdot m^{A'}}M + F_s \cdot \delta\langle r^2\rangle^{A,A'} \quad . \quad (2)$$

The constants M and F_s were determined by atomic calculations as summarized in Table I. The obtained changes in mean square charge radii for the nobelium isotopes in comparison to experimental values for other actinides [36, 37] are shown in Fig. 2. The experimental results for different actinide isotopes agree well with calculated values from self-consistent nuclear density functional theory (DFT) without any symmetry restrictions [38] for even-even nuclides obtained with two Skyrme functionals. An alternative to the Skyrme functionals are the

Fayans functionals, which recently have been optimized with a focus on charge radii [39]. However, those functionals overestimate the pairing correlations particularly in the actinide region, which could have a significant influence on the results. The proton density distribution for ^{254}No predicted by UNEDF1 is shown in Fig. 3. The calculated distribution clearly indicates the deformation as well as a central depression, which originates from the strong Coulomb repulsion (see, e.g., [2, 40, 41]). The maximum in quadrupole deformation, defined by the deformation parameter β_2, is predicted by the DFT calculations to be around $N = 148$ as shown in the upper panel in Fig. 3. For the nobelium isotopes this results in a deformation parameter which only changes slightly for the investigated isotopes. This is in line with other calculations [4, 42, 43], experimental results from in-beam gamma spectroscopy of ^{252,254}No [7, 44] and the spectroscopic quadrupole moment from our HFS measurements in ^{253}No. The effect of the deformation with respect to on the central depression is illustrated in the lower panel in Fig. 3. The relative depth of the central depression, defined as $(\rho_\mathrm{max} - \rho_\mathrm{c})/\rho_\mathrm{max}$ with the maximum proton density ρ_max and the proton density in the center ρ_c, increases with an increasing deformation parameter which leads to an additional contribution to the charge radii. In general our experimental results are in good agreement with DFT calculations. For comparison the results of $\delta\langle r^2\rangle$ from a parameterization of a droplet model (DM) [45, 46] for stable deformation, as typically done in laser spectroscopic investigations up to the lead region [11], is shown for $Z = 90$–102 in Fig. 2 as a gray area. Typically, a deviation from this slope is attributed to changes in deformation, but the experimental values for nuclei around the maximum in deformation continue to deviate. This indicates that the increase in charge radii, potentially

from the central depression of the charge redistribution, is underestimated by the DM in this region of high Z and strongly deformed nuclei. ~~It is also worth noting that a parametrization of a droplet model (DM) [45, 46], as typically done in laser spectroscopic investigations up to the lead region [11], is not suitable for the investigated isotopes. The lines for a stable deformation from the DM for $Z = 90$-102 are shown in Fig. 2 as a gray area. A steady deviation from this slope for all nuclei around a maximum in deformation indicates that the increase in charge radii, potentially from the central depression of the charge redistribution is underestimated by the DM in this region of high Z and strongly deformed nuclei.~~ In summary, nuclear ground-state properties were obtained from laser spectroscopy for the nobelium isotopes ^{252,253,254}No. The results are the first of their kind in the transfermium region, where elements are available in single atom-at-a-time quantities only. Besides the first experimental determination of the magnetic dipole and spectroscopic quadrupole moment of ^{253}No, the results of the isotope shift match well with changes in mean square charge radii calculated by nuclear DFT, which predict a strong central depression in the charge density of more than 12%. Laser spectroscopy, in combination with state-of-the art atomic calculations, can now also be employed to study the structure of K-isomers and the properties of deformed nuclei in the heavy element region around nobelium, which forms the basis for a better understanding of the nuclear structure of the heaviest elements.

* s.raeder@gsi.de
† present address: Max-Planck-Institut für Kernphysik, 69120 Heidelberg, Germany.

[1] Z. Patyk, A. Sobiczewski, P. Armbruster, and K.-H. Schmidt, Nucl. Phys. A **491**, 267 (1989).
[2] B. Schuetrumpf, W. Nazarewicz, and P.-G. Reinhard, Phys. Rev. C **96**, 024306 (2017).
[3] M. G. Mayer and J. H. D. Jensen, *Elementary theory of nuclear shell structure* (Wiley, 1964).
[4] P.-H. Heenen, J. Skalski, A. Staszczak, and D. Vretenar, Nucl. Phys. A **944**, 415 (2015).
[5] R.-D. Herzberg, P. Greenlees, P. Butler, G. Jones, M. Venhart, I. Darby, S. Eeckhaudt, K. Eskola, T. Grahn, C. Gray-Jones, *et al.*, Nature **442**, 896 (2006).
[6] S. K. Tandel, T. L. Khoo, D. Seweryniak, G. Mukherjee, I. Ahmad, B. Back, R. Blinstrup, M. P. Carpenter, J. Chapman, P. Chowdhury, C. N. Davids, A. A. Hecht, A. Heinz, P. Ikin, R. V. F. Janssens, F. G. Kondev, T. Lauritsen, C. J. Lister, E. F. Moore, D. Peterson, P. Reiter, U. S. Tandel, X. Wang, and S. Zhu, Phys. Rev. Lett. **97**, 082502 (2006).
[7] P. Reiter, T. L. Khoo, C. J. Lister, D. Seweryniak, I. Ahmad, M. Alcorta, M. P. Carpenter, J. A. Cizewski, C. N. Davids, G. Gervais, J. P. Greene, W. F. Henning, R. V. F. Janssens, T. Lauritsen, S. Siem, A. A. Sonzogni, D. Sullivan, J. Uusitalo, I. Wiedenhöver, N. Amzal, P. A. Butler, A. J. Chewter, K. Y. Ding, N. Fotiades, J. D. Fox, P. T. Greenlees, R.-D. Herzberg, G. D. Jones, W. Korten, M. Leino, and K. Vetter, Phys. Rev. Lett. **82**, 509 (1999).
[8] M. Leino, H. Kankaanää, R.-D. Herzberg, A. Chewter, F. Heßberger, Y. Le Coz, F. Becker, P. Butler, J. Cocks, O. Dorvaux, K. Eskola, J. Gerl, P. Greenlees, K. Helariutta, M. Houry, G. Jones, P. Jones, R. Julin, S. Juutinen, H. Kettunen, T. Khoo, A. Kleinböhl, W. Korten, P. Kuusiniemi, R. Lucas, M. Muikku, P. Nieminen, R. Page, P. Rahkila, P. Reiter, A. Savelius, C. Schlegel, C. Theisen, W. Trzaska, and H.-J. Wollersheim, Europ. Phys. J. A **6**, 63 (1999).
[9] P. T. Greenlees, J. Rubert, J. Piot, B. J. P. Gall, L. L. Andersson, M. Asai, Z. Asfari, D. M. Cox, F. Dechery, O. Dorvaux, T. Grahn, K. Hauschild, G. Henning, A. Herzan, R.-D. Herzberg, F. P. Heßberger, U. Jakobsson, P. Jones, R. Julin, S. Juutinen, S. Ketelhut, T.-L. Khoo, M. Leino, J. Ljungvall, A. Lopez-Martens, R. Lozeva, P. Nieminen, J. Pakarinen, P. Papadakis, E. Parr, P. Peura, P. Rahkila, S. Rinta-Antila, P. Ruotsalainen, M. Sandzelius, J. Sarén, C. Scholey, D. Seweryniak, J. Sorri, B. Sulignano, C. Theisen, J. Uusitalo, and M. Venhart, Phys. Rev. Lett. **109**, 012501 (2012).
[10] C. Theisen, P. Greenlees, T.-L. Khoo, P. Chowdhury, and T. Ishii, Nucl. Phys. A **944**, 333 (2015).
[11] P. Campbell, I. Moore, and M. Pearson, Prog. Part. Nucl. Phys. **86**, 127 (2016).
[12] M. Laatiaoui, W. Lauth, H. Backe, M. Block, D. Ack-

ermann, B. Cheal, P. Chhetri, C. E. Düllmann, P. van Duppen, J. Even, R. Ferrer, F. Giacoppo, S. Götz, F. P. Heßberger, M. Huyse, O. Kaleja, J. Khuyagbaatar, P. Kunz, F. Lautenschläger, A. K. Mistry, S. Raeder, E. Minaya Ramirez, T. Walther, C. Wraith, and A. Yakushev, Nature **538**, 495 (2016).

[13] H. Backe, W. Lauth, M. Block, and M. Laatiaoui, Nucl. Phys. A **944**, 492 (2015).

[14] F. Lautenschläger, P. Chhetri, D. Ackermann, H. Backe, M. Block, B. Cheal, A. Clark, C. Droese, R. Ferrer, F. Giacoppo, S. Götz, F. Heßberger, O. Kaleja, J. Khuyagbaatar, P. Kunz, A. Mistry, M. Laatiaoui, W. Lauth, S. Raeder, T. Walther, and C. Wraith, Nucl. Instrum. Meth. Phys. Res. B **383**, 115 (2016).

[15] Y. T. Oganessian, V. K. Utyonkov, Y. V. Lobanov, F. S. Abdullin, A. N. Polyakov, I. V. Shirokovsky, Y. S. Tsyganov, A. N. Mezentsev, S. Iliev, V. G. Subbotin, A. M. Sukhov, K. Subotic, O. V. Ivanov, A. N. Voinov, V. I. Zagrebaev, K. J. Moody, J. F. Wild, N. J. Stoyer, M. A. Stoyer, and R. W. Lougheed, Phys. Rev. C **64**, 054606 (2001).

[16] G. Münzenberg, W. Faust, S. Hofmann, P. Armbruster, K. Güttner, and H. Ewald, Nucl. Instrum. Meth. **161**, 65 (1979).

[17] M. Laatiaoui, H. Backe, M. Block, F.-P. Heßberger, P. Kunz, F. Lautenschläger, W. Lauth, M. Sewtz, and T. Walther, Europ. Phys. J. D **68**, 1 (2014).

[18] M. Laatiaoui, H. Backe, M. Block, P. Chhetri, F. Lautenschläger, W. Lauth, and T. Walther, Hyperfine Interact. **227**, 69 (2014).

[19] P. Chhetri, D. Ackermann, H. Backe, M. Block, B. Cheal, C. E. Düllmann, J. Even, R. Ferrer, F. Giacoppo, S. Götz, F. P. Heßberger, O. Kaleja, J. Khuyagbaatar, P. Kunz, M. Laatiaoui, F. Lautenschläger, W. Lauth, E. M. Ramirez, A. K. Mistry, S. Raeder, C. Wraith, T. Walther, and A. Yakushev, Europ. Phys. J. D **71**, 195 (2017).

[20] M. S. Safronova, M. G. Kozlov, W. R. Johnson, and D. Jiang, Phys. Rev. A **80**, 012516 (2009).

[21] V. A. Dzuba, Phys. Rev. A **90**, 012517 (2014).

[22] V. A. Dzuba, V. V. Flambaum, and M. G. Kozlov, Phys. Rev. A **54**, 3948 (1996).

[23] J. C. Berengut, V. V. Flambaum, and M. G. Kozlov, Phys. Rev. A **73**, 012504 (2006).

[24] E. Eliav, S. Fritzsche, and U. Kaldor, Nucl. Phys. A **944**, 518 (2015), special Issue on Superheavy Elements.

[25] P. Jönsson, X. He, C. F. Fischer, and I. Grant, Comput. Phys. Commun. **177**, 597 (2007).

[26] I. P. Grant, *Relativistic quantum theory of atoms and molecules: theory and computation*, Vol. 40 (Springer Science & Business Media, 2007).

[27] V. A. Dzuba, J. C. Berengut, C. Harabati, and V. V. Flambaum, Phys. Rev. A **95**, 012503 (2017).

[28] F. P. Heßberger, S. Hofmann, D. Ackermann, P. Cagarda, R. D. Herzberg, I. Kojouharov, P. Kuusiniemi, M. Leino, and R. Mann, Europ. Phys. J. A **22**, 417 (2004).

[29] A. K. Mistry, R. D. Herzberg, P. Greenlees, P. Papadakis, K. Auranen, P. A. Butler, D. M. Cox, A. B. Garnsworthy, T. Grahn, K. Hauschild, U. Jakobsson, D. T. Joss, R. Julin, S. Ketelhut, J. Konki, M. Leino, A. Lopez-Martens, R. D. Page, J. Pakarinen, P. Peura, P. Rahkila, M. Sandzelius, C. Scholey, J. Simpson, D. Seddon, J. Sorri, S. Stolze, J. Thornhill, J. Uusitalo, and D. Wells, Europ. Phys. J. A **53**, 24 (2017).

[30] H. Backe, A. Dretzke, S. Fritzsche, R. G. Haire, P. Kunz, W. Lauth, M. Sewtz, and N. Trautmann, Hyperfine Interact. **162**, 3 (2005).

[31] A. Bohr and B. R. Mottelson, *Nuclear Structure, Volume I: Single-Particle Motion; Volume II: Nuclear Deformations* (World Scientific, 1998).

[32] R. D. Herzberg, S. Moon, S. Eeckhaudt, P. T. Greenlees, P. A. Butler, T. Page, A. V. Afanasjev, N. Amzal, J. E. Bastin, F. Becker, M. Bender, B. Bruyneel, J. F. C. Cocks, I. G. Darby, O. Dorvaux, K. Eskola, J. Gerl, T. Grahn, C. Gray-Jones, N. J. Hammond, K. Hauschild, P. H. Heenen, K. Helariutta, A. Herzberg, F. Hessberger, M. Houry, A. Hürstel, R. D. Humphreys, G. D. Jones, P. M. Jones, R. Julin, S. Juutinen, H. Kankaanpää, H. Kettunen, T. L. Khoo, W. Korten, P. Kuusiniemi, Y. LeCoz, M. Leino, A. P. Leppänen, C. J. Lister, R. Lucas, M. Muikku, P. Nieminen, M. Nyman, R. D. Page, T. Page, J. Pakarinen, A. Pritchard, P. Rahkila, P. Reiter, M. Sandzelius, J. Saren, C. Schlegel, C. Scholey, C. Theisen, W. H. Trzaska, J. Uusitalo, A. Wiens, and H. J. Wollersheim, Europ. Phys. J. A **42**, 333 (2009).

[33] P. Reiter, T. L. Khoo, I. Ahmad, A. V. Afanasjev, A. Heinz, T. Lauritsen, C. J. Lister, D. Seweryniak, P. Bhattacharyya, P. A. Butler, M. P. Carpenter, A. J. Chewter, J. A. Cizewski, C. N. Davids, J. P. Greene, P. T. Greenlees, K. Helariutta, R.-D. Herzberg, R. V. F. Janssens, G. D. Jones, R. Julin, H. Kankaanpää, H. Kettunen, F. G. Kondev, P. Kuusiniemi, M. Leino, S. Siem, A. A. Sonzogni, J. Uusitalo, and I. Wiedenhöver, Phys. Rev. Lett. **95**, 032501 (2005).

[34] M. Kortelainen, J. McDonnell, W. Nazarewicz, P.-G. Reinhard, J. Sarich, N. Schunck, M. V. Stoitsov, and S. M. Wild, Phys. Rev. C **85**, 024304 (2012).

[35] P. Klüpfel, P. G. Reinhard, T. J. Bürvenich, and J. A. Maruhn, Phys. Rev. C **79**, 034310 (2009).

[36] I. Angeli and K. Marinova, Atom. Data Nucl. Data Tab. **99**, 69 (2013).

[37] A. Voss, V. Sonnenschein, P. Campbell, B. Cheal, T. Kron, I. D. Moore, I. Pohjalainen, S. Raeder, N. Trautmann, and K. Wendt, Phys. Rev. A **95**, 032506 (2017).

[38] J. A. Maruhn, P.-G. Reinhard, P. D. Stevenson, and A. S. Umar, Comput. Phys. Commun. **185**, 2195 (2014).

[39] P.-G. Reinhard and W. Nazarewicz, Phys. Rev. C **95**, 064328 (2017).

[40] W. D. Myers and W. J. Swiatecki, Ann. Phys. **55**, 395 (1969).

[41] P. Möller, J. Nix, W. D. Myers, and W. J. Swiatecki, Nucl. Phys. A **536**, 61 (1992).

[42] P. Möller, J. Nix, W. Myers, and W. Swiatecki, Atom. Data Nucl. Data Tab. **59**, 185 (1995).

[43] A. Sobiczewski, I. Muntian, and Z. Patyk, Phys. Rev. C **63**, 034306 (2001).

[44] R.-D. Herzberg, N. Amzal, F. Becker, P. A. Butler, A. J. C. Chewter, J. F. C. Cocks, O. Dorvaux, K. Eskola, J. Gerl, P. T. Greenlees, N. J. Hammond, K. Hauschild, K. Helariutta, F. Heßberger, M. Houry, G. D. Jones, P. M. Jones, R. Julin, S. Juutinen, H. Kankaanpää, H. Kettunen, T. L. Khoo, W. Korten, P. Kuusiniemi, Y. LeCoz, M. Leino, C. J. Lister, R. Lucas, M. Muikku, P. Nieminen, R. D. Page, P. Rahkila, P. Reiter, C. Schlegel, C. Scholey, O. Stezowski, C. Theisen, W. H. Trzaska, J. Uusitalo, and H. J. Wollersheim, Phys. Rev. C **65**, 014303 (2001).

[45] W. D. Myers and K.-H. Schmidt, Nucl. Phys. A **410**, 61 (1983).

[46] D. Berdichevsky and F. Tondeur, Z. Phys. A **322**, 141 (1985).